

Supplementary Materials for

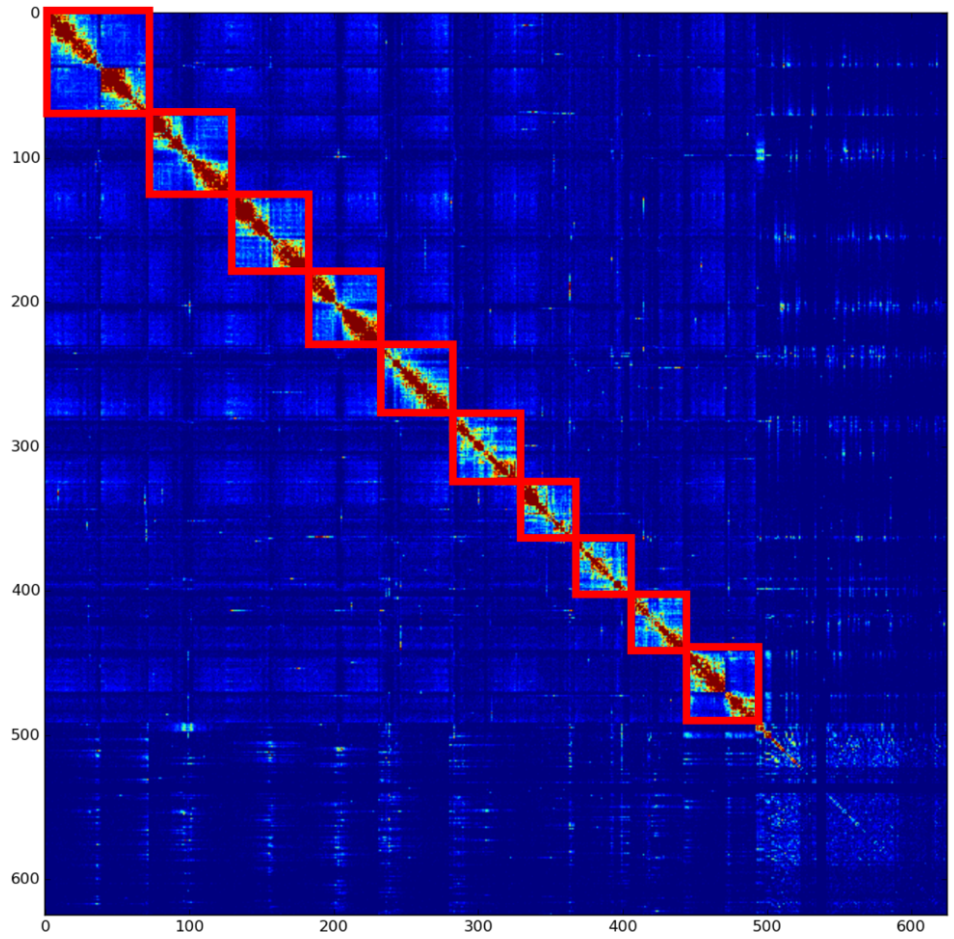
**Chromosomal scale genome assembly reveals symbiotic virus colonization of parasitic wasp DNA**

J. Gauthier, H. Boulain, J. J.F.A. van Vugt, L. Baudry, E. Persyn, J.-M. Aury, B. Noel, A. Bretaudeau, F. Legeai, S. Warris, M. A. Chebbi, G. Dubreuil, B. Duvic, N. Kremer, P. Gayral, K. Musset, T. Josse, D. Bigot, C. Bressac, S. Moreau, G. Periquet, M. Harry, N. Montagné, I. Boulogne, M. Sabeti-Azad, M. Maïbèche, T. Chertemps, F. Hilliou, D. Siaussat, J. Amsellem, I. Luyten, C. Capdevielle-Dulac, K. Labadie, B. Laïs Merlin, V. Barbe, J. G. de Boer, M. Marbouty, F. L. Cònsoli, S. Dupas, A. Hua Van, G. Le Goff, A. Bézier, E. Jacquin-Joly, J. B. Whitfield, L.E.M. Vet, H. M. Smid, L. Kaiser-Arnault, R. Koszul, E. Huguet, E. A. Herniou and J.-M. Drezen\* .

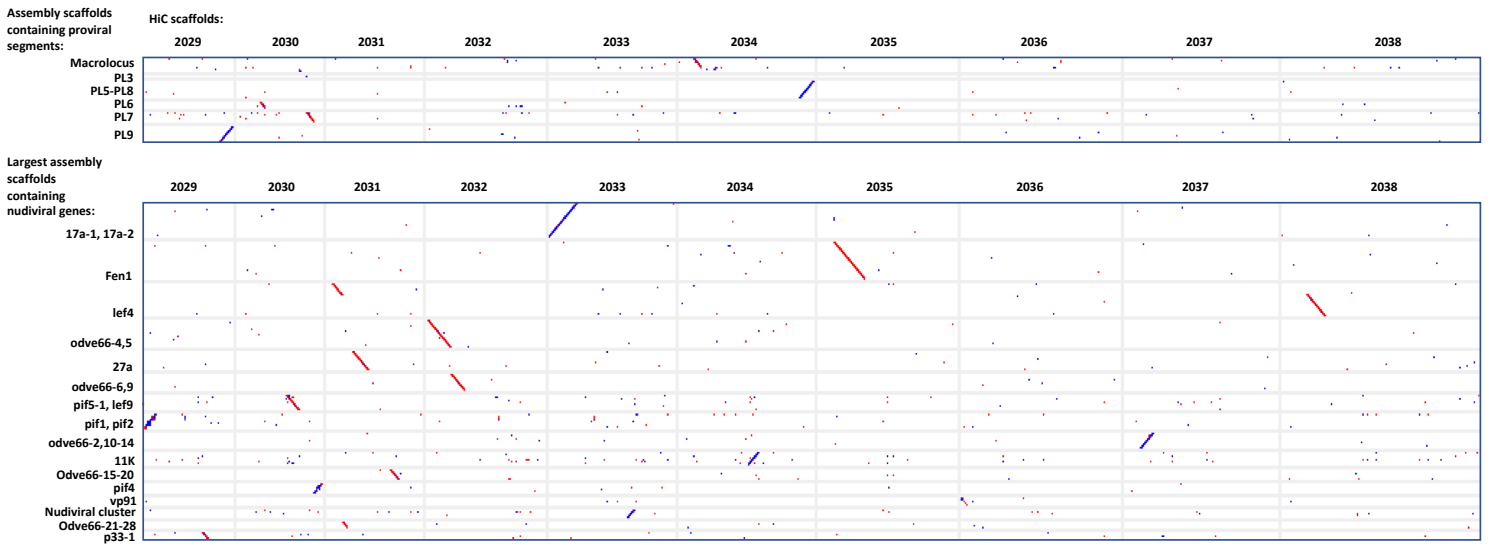
\*corresponding author: drezen@univ-tours.fr

A

chromosome 1  
 chromosome 2  
 chromosome 3  
 chromosome 4  
 chromosome 5  
 chromosome 7  
 chromosome 6  
 chromosome 8  
 chromosome 9  
 chromosome 10

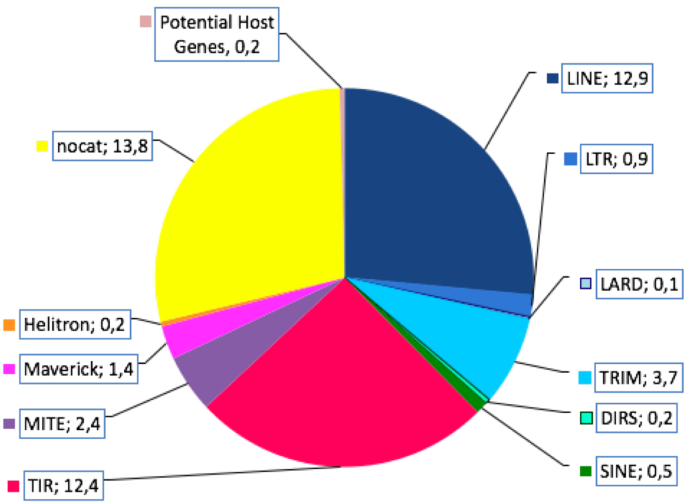


B

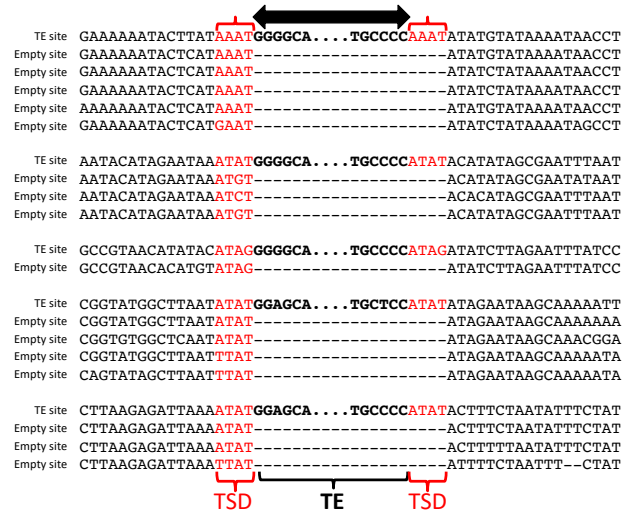


**Supplementary Figure 1. A** Contact matrix between each fragment used for the GRAAL assembly, from blue the most distant to red the closest fragments. Along the two axis the fragments are organized according to this distance. The red frames have been added to visualize the chromosomes separations. The assignment of each chromosome has been performed using the chromosome length and centromere positions but also including sequences used for *in situ* hybridization performed by Belle and colleagues (doi:10.1128/JVI.76.11.5793-5796.2002) **B** Dot plot: assembly scaffolds containing bracovirus sequences/HiC scaffolds. Assembly scaffolds are confirmed by HiC scaffolds (except for the *lef4*-containing scaffold which is split in two pieces in HiC).

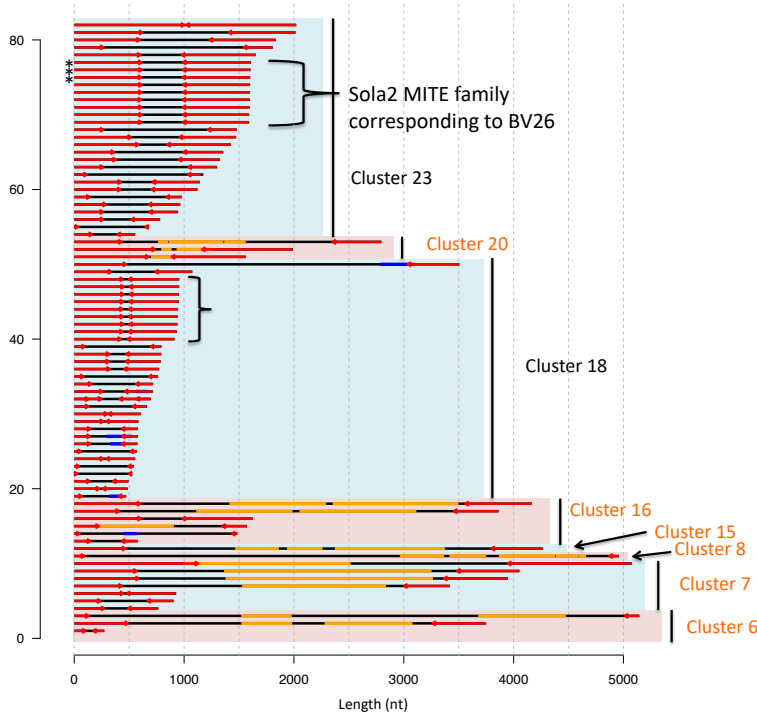
A



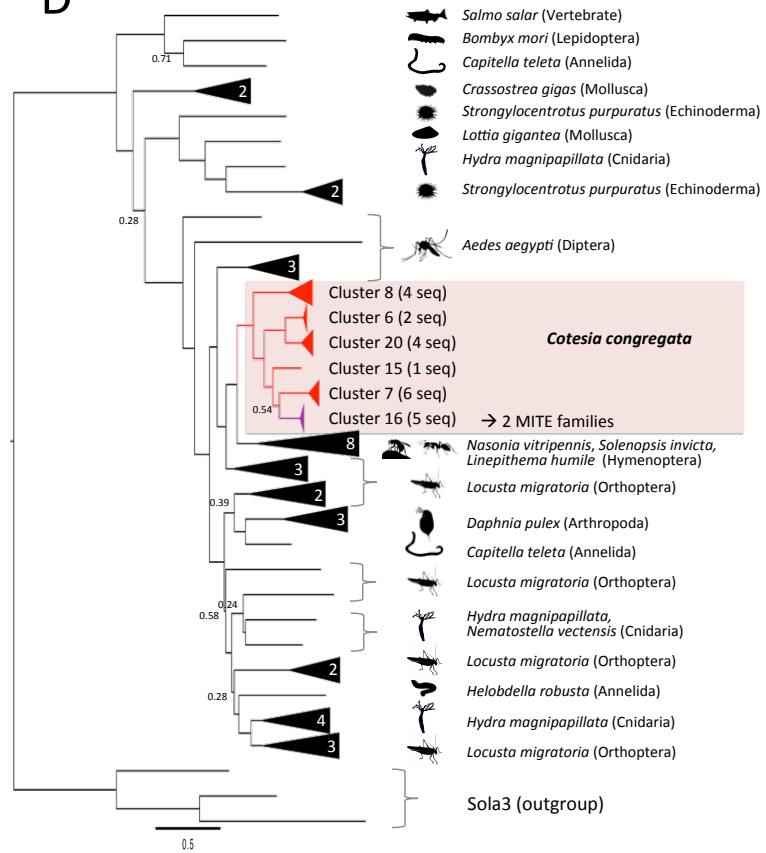
C



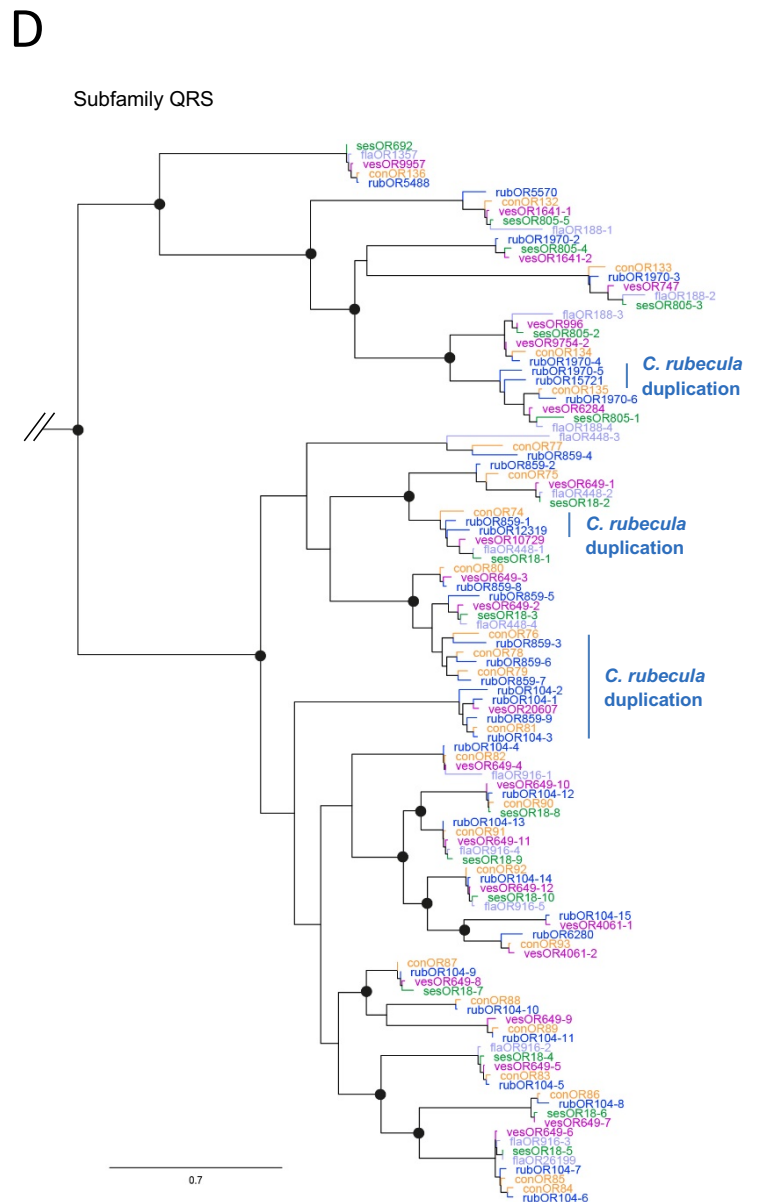
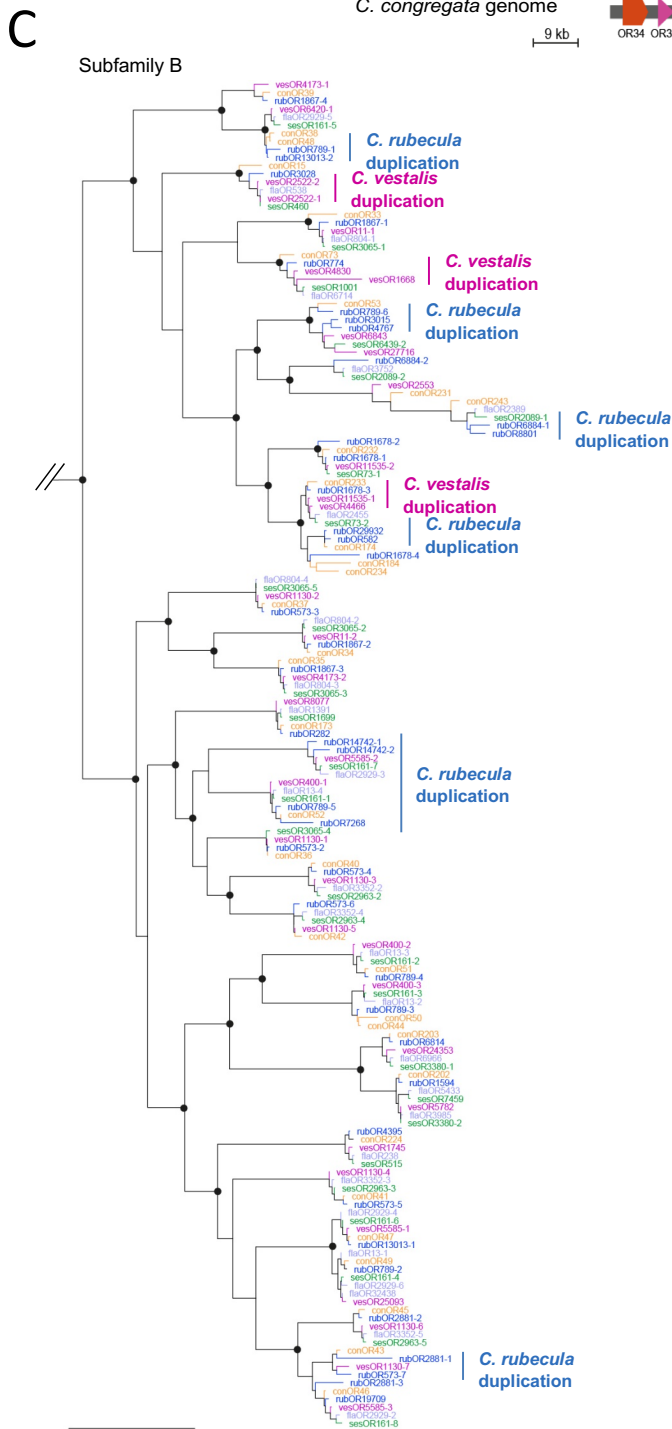
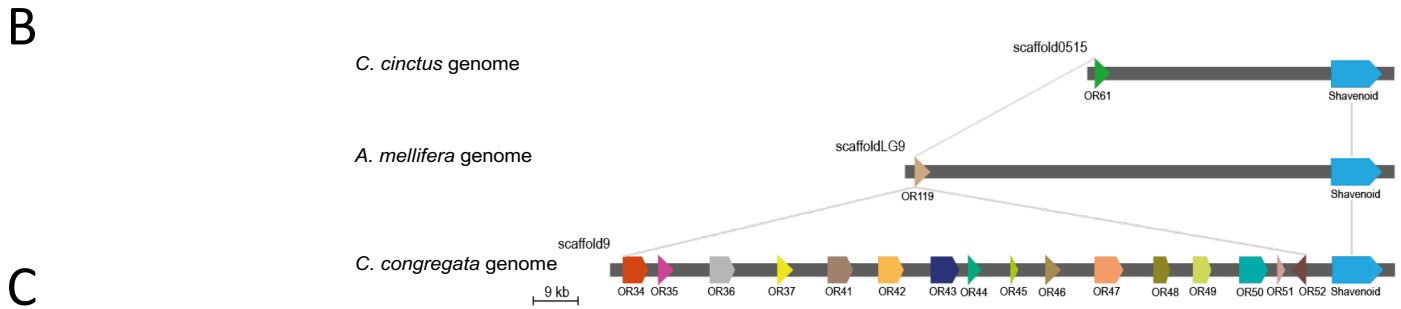
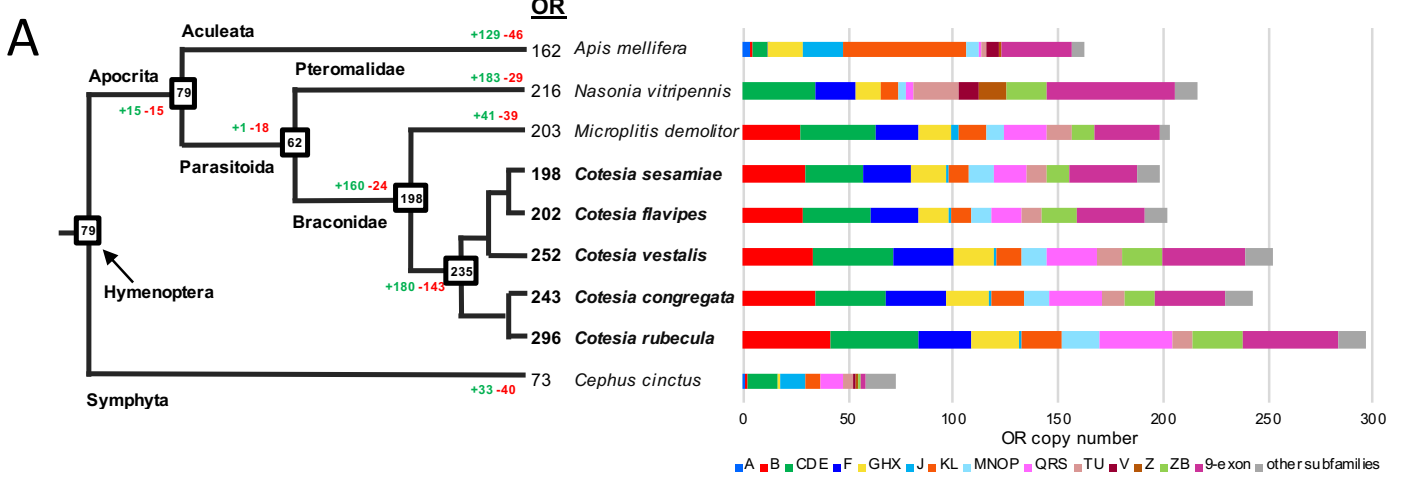
B



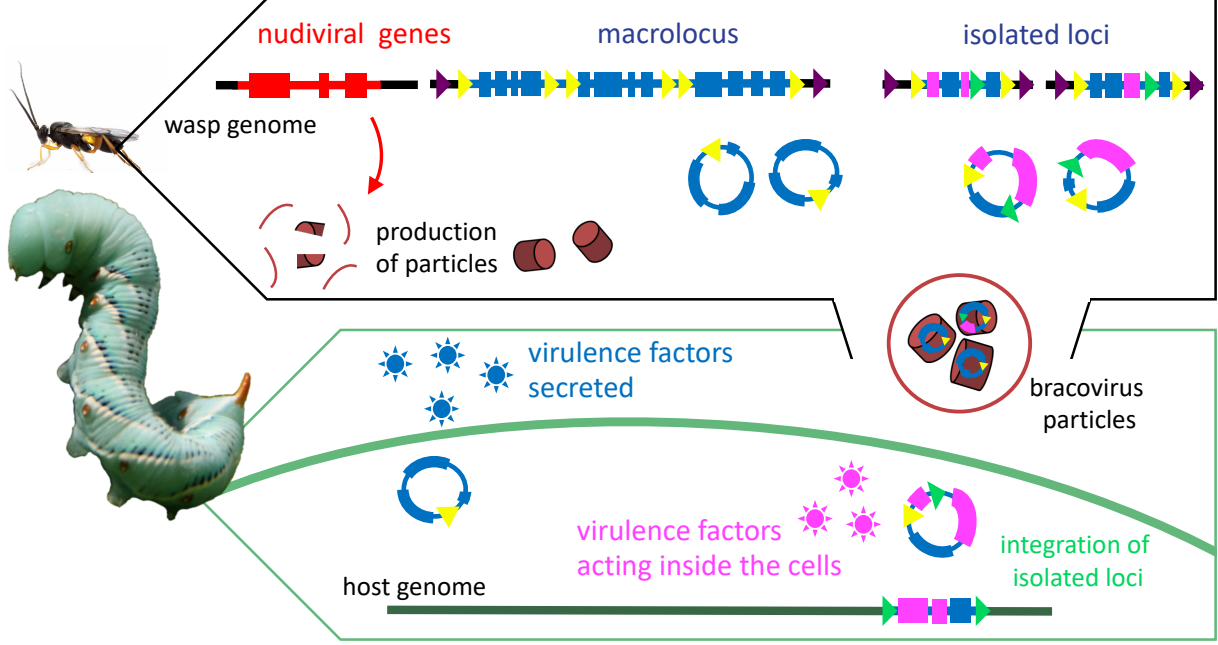
D



**Supplementary Figure 2.** REPET annotation of transposable elements and characteristics of Sola2 elements at the origin of bracovirus virulence genes BV26. **A** Pie plot of transposable elements organized by families, as detected by REPET. **B** Structure of the Sola2 family. BV26 corresponds to a MITE (Miniature Inverted-repeat Transposable Element), 1606 bp long with 616 nt TIR (Terminal Inverted Repeats) related to the TIR of a Sola2 family (BLASTN). 82 related sequences were grouped into 8 clusters (usearch v5.1 (<http://www.drive5.com/usearch>) -id=0.8). Six clusters (name in orange) contained sequences with homology to Sola2 transposase (orange part) (blastx against RepBase20.05\_REPET edition, -evalue 1e-4). Blue parts indicate homology with other TEs from RepBase. Red arrows represent the TIRs of the elements. The two most abundant correspond to 2 MITE clusters and copies resulting from amplification (same size and sequences) are highlighted by brackets. The asterisks indicates the 3 copies previously annotated as bracovirus genes BV26. **C** Graph showing the target site duplication (4-nt, TA rich) produced during element insertion deduced from the comparison of some Sola2 insertions sites with paralogous empty sites. As for typical Sola2 element, TIRs start by G-rich sequences. **D** Phylogenetic tree showing the relationships between Sola2 translated sequences from *C. congregata* (framed branches) and other Sola2 transposases from RepBase. The alignment (MAFFT v7 (<https://mafft.cbrc.jp/alignment/software/>)) was truncated to keep only the 250 AA-long best conserved part (AA 240 to 520 of Sola2-1\_Nvi) for a phylogenetic analysis using FastTree (<http://www.microbesonline.org/fasttree/>). Black triangles group TE consensus sequences from the same species (number of sequences is indicated). Open triangles represent consensus sequences of Sola3 elements (RepBase) used as an outgroup. Numbers on the branches are the robustness (local bootstraps) as implemented in FastTree. One group (purple) may be at the origin of the 2 MITEs families (based on TIR similarities). The resulting tree suggests a monophyletic origin of the *C. congregata* Sola2 sequences. Our knowledge of Sola2 elements remains fragmentary, only few genomes having been screened. Closest sequences in Repbase are found in the related parasitoid *Nasonia vitripennis*, and two ant species. Potentially active sequences (long ORFs, no stop codons or frameshift, with one intron) could be identified in clusters 6 and 16.



**Supplementary Figure 3.** **A** Copy number dynamics of OR genes in five *Cotesia* species and four other Hymenoptera species. Estimated numbers of gene gain and loss events are shown on each branch of the species tree in green and red, respectively. The size of OR repertoires in common ancestors is indicated in boxes at the corresponding nodes of the species tree. The histogram represents the distribution of OR copy number per subfamily for each species. **B** Synteny among the OR subfamily B in *C. congregata*, *C. cinctus* and *A. mellifera*, based on inter-specific conservation of the shavenoid gene, showing expansion through tandem duplications for *C. congregata* OR genes. Orientation (arrows) of genes within scaffolds are indicated. **C** and **D** phylogenies OR subfamilies B and QRS respectively in five *Cotesia* species. These subtrees were extracted from maximum-likelihood phylogeny of *Cotesia* ORs including OR repertoires from *C. congregata* (orange), *C. flavipes* (purple), *C. rubecula* (blue), *C. sesamiae* (green) and *C. vestalis* (pink). The tree was rooted using the Orco clade as outgroup. Circles indicate nodes strongly supported by the approximate likelihood-ratio test ( $aLRT \geq 0.95$ ). The scale bar represents 0.7 expected amino acid substitutions per site. *C. rubecula* and *C. vestalis* duplicated gene copies are indicated on the right.

**A****B**

▶ Replication Unit Motif    
 ▶ DRJ    
 ▶ Host Integration Motif

### Replication Unit Motif Type 1 Head

```

CC_RUM_T1_H_LP1_SEG-1  CCGGATTCGGATATGTGGAAACCTACTGTGAAG...
CC_RUM_T1_H_LP4_SEG-7  AGAATCCGTTTACGGATTAACCTACTGTGAAG...
CC_RUM_T1_H_LP5_SEG-1  CGCCACGGATTCGGGARGTTACTGTAGTGAT...
CC_RUM_T1_H_LP7_SEG-4  TCTGCTTGGATATGGATTTTACTGTAATAGT...
CC_RUM_T1_H_LP8_SEG-26  TTTTATTAGATTAAAGAGACTTACTG...
MD_RUM_T1_H_LP3_SEG-6  AACATCCGGATACGGCGTATTTACTGTAGT...
MD_RUM_T1_H_LP3_SEG-N  TACATTCGGATACGGGATCTTACTGTAGT...
MD_RUM_T1_H_LP4_SEG-H  AATCCGGATATCGGATGATTTACTGTAGT...
MD_RUM_T1_H_LP6_SEG-5  TACCTTCGGATATCGGATGATTTACTGTAGT...
MD_RUM_T1_H_LP8_SEG-U  GATGTCGGATAAAGAGGCTTACTGTAGT...
  
```

### Replication Unit Motif Type 1 Tail

```

CC_RUM_T1_T_LP3_SEG-7  TAAACAATTTGTCATAATTTTACAAATTTT...
CC_RUM_T1_T_LP4_SEG-7  TTAATAAACCTGGATAAATTTTCTCGA...
CC_RUM_T1_T_LP5_SEG-1  ACTAGATGATGATAAATTTTCTATAAAT...
CC_RUM_T1_T_LP8_SEG-26  TATTTTAAAGGATATAAATTTTCTATAA...
MD_RUM_T1_T_LP3_SEG-6  ACTGTAGTATGATATAAATTTTCTATAA...
MD_RUM_T1_T_LP3_SEG-N  ACTGTAGTATGATATAAATTTTCTATAA...
MD_RUM_T1_T_LP4_SEG-H  TBCATAGTATGATATAAATTTTCTATAA...
MD_RUM_T1_T_LP6_SEG-5  AAACCTGGATGATATAAATTTTCTATAA...
MD_RUM_T1_T_LP8_SEG-U  ACTGTAGTATGATATAAATTTGATTC...
  
```

### Replication Unit Motif Type 2 Head

```

CC_RUM_T2_H_L9_PART-2  TTTGGGATGATGGTAAACCTTA...
CC_RUM_T2_H_L11_PART-2  TTTGGGATGATGGTAAACCTTA...
CC_RUM_T2_H_L12_PART-1  TTTGGGATGATGGTAAACCTTA...
CC_RUM_T2_H_L12_PART-2  TTTGGGATGATGGTAAACCTTA...
CC_RUM_T2_H_L12_PART-3  TTTGGGATGATGGTAAACCTTA...
MD_RUM_T2_H_L11_SEG-0  TTTGGGATGATGGTAAACCTTA...
MD_RUM_T2_H_L11_SEG-P  AACCTGGATGATGGTAAACCTTA...
MD_RUM_T2_H_L11_SEG-V  TTTGGGATGATGGTAAACCTTA...
MD_RUM_T2_H_L15_SEG-8  CTCGGGACAAACGGAGGCTTA...
MD_RUM_T2_H_L17_SEG-T  ATCTGGATATATGGGACCTTA...
  
```

### Replication Unit Motif Type 2 Tail

```

CC_RUM_T2_T_PL2_PART-4  GAAGAAATTTATAAATTTTATTCGCT...
CC_RUM_T2_T_PL2_PART-5  TTAATTAATAAATTTAATAAATTTT...
CC_RUM_T2_T_PL2_PART-6  TTAATTAATAAATTTAATAAATTTT...
CC_RUM_T2_T_PL6_PART-1  AAATTTTAAATTTTAAATTTTAAAT...
CC_RUM_T2_T_PL6_PART-2  ATGAATGAATTTTAAATTTTAAAT...
CC_RUM_T2_T_PL6_PART-3  TAAATTAATAAATTTTAAATTTTAAAT...
MD_RUM_T2_T_PL1_SEG-0  AATTTGATTAATAAATTTAATAAAT...
MD_RUM_T2_T_PL2_SEG-X  TTAATAAATAAATTTAATAAAT...
MD_RUM_T2_T_PL5_SEG-R  TTTGAATTAATTTTAAATTTAATAA...
MD_RUM_T2_T_PL7_SEG-T  GAAATTTGCTTCATATAAATTTCA...
  
```

### DRJ Circle

```

CC_DRJ_CIRCLE-1  TGAATTTAACTTTGAATATTTTCCCTACTCGAGATTTGTGGAGATTAATACGAATAG...
CC_DRJ_CIRCLE-10  TGAATTTAACTTTGAATATTTTCCCTACTCGAGATTTGTGGAGATTAATACGAATAG...
CC_DRJ_CIRCLE-11  TGAATTTAAAGACTCGATTTGTAGTGAATAAACATGTTAAGGTCCGATTTGTTTAT...
CC_DRJ_CIRCLE-12  TGAATTTAAAGTTTAAAGTTTCTAATTTATGTAAGACATGTAAAGATTTAATTTG...
CC_DRJ_CIRCLE-13  TGAATTTAAAGAAAGACTAATTTGTGACTAGGCGCTGGATTAAGATTTCCAAATC...
CC_DRJ_CIRCLE-14  TGAATTTAAATACAGTAAATTTGCGGCTGGAGGAAACAAAGTATGGAATGGA...
CC_DRJ_CIRCLE-15  TGAATTTAAATACAGTAAATTTGCGGCTGGAGGAAACAAAGTATGGAATGGA...
CC_DRJ_CIRCLE-16  TGAATTTAAATCGTGCATAAATGTTGACRATCTATAGATCAAAAATGTTAGCT...
CC_DRJ_CIRCLE-17  TGAATTTAAATCGTGCATAAATGTTGACRATCTATAGATCAAAAATGTTAGCT...
CC_DRJ_CIRCLE-18  TGAATTTGCAAGCATCTAATTTGTTAATTTTATGCGCTTCTTTAGTAAGAT...
CC_DRJ_CIRCLE-19  TGAATTTAAAGAAAGATTAATAAGCAAGAGGATTTGCGCTAAAGATCTTA...
CC_DRJ_CIRCLE-20  TGAATTTAAATGATGAATTAATGATCTAGAGTAAACAAATGAAAGATTTT...
CC_DRJ_CIRCLE-21  TGAATTTAAATGATGAATTAATGATCTAGAGTAAACAAATGAAAGATTTT...
CC_DRJ_CIRCLE-22  TGAATTTGGGTAATGAATTAATGTTGCTAAAGCATGATCTAATAAGGAT...
CC_DRJ_CIRCLE-23  TGAATTTAAAGAAAGATTAATAAGCAAGGATTTGCGCTAAAGATCTTA...
CC_DRJ_CIRCLE-24  TGAATTCAGGATGGTTTATAAABEGCAATTTTCCGCTTAAGAGAGTTA...
CC_DRJ_CIRCLE-25  TGAATTTAAATGATGATTAAGATCTCAATACGGTAAATTTAATGATTA...
CC_DRJ_CIRCLE-26  TGAATTTAAAGCTTATTCATTTGTTTCAATAGCGATTAATAAAGAT...
CC_DRJ_CIRCLE-27  TGAATTCAGGATGGTTTATAAABEGCAATTTTCCGCTTAAGAGAGTTA...
CC_DRJ_CIRCLE-28  TGAATTTAAAGAAAGATTAATAAGCAAGGATTTGCGCTAAAGATCTTA...
CC_DRJ_CIRCLE-29  TGAATTCAGGATGGTTTATAAABEGCAATTTTCCGCTTAAGAGAGTTA...
CC_DRJ_CIRCLE-30  TGAATTTAAACGAAAGCAATAAAGTGTCAAGATGAGCTTAAAGAT...
CC_DRJ_CIRCLE-31  TGAATTTTAAATGATGAATTAATGATCTAGAGTAAACAAATGAAAGAT...
CC_DRJ_CIRCLE-32  TGAATTTGACAGCATCTAATTTGGTAAATTTTACCGCTTCTTTAGTAAG...
CC_DRJ_CIRCLE-33  TGAATTTAAAGAAAGATTAATAAGCAAGGATTTGCGCTAAAGATCTTA...
CC_DRJ_CIRCLE-34  TGAATTTGATTAACACGATCAAAATCGCGCTGGGAAACAAATGATGGA...
CC_DRJ_CIRCLE-35  TGAATTTGATTAACACGATCAAAATCGCGCTGGGAAACAAATGATGGA...
CC_DRJ_CIRCLE-36  TGAATTTGGGTAATGAATTAATGTTGCTAAAGCATGATCTAATAAGGAT...
CC_DRJ_CIRCLE-37  TGAATTTGATTAACACGATCAAAATCGCGCTGGGAAACAAATGATGGA...
CC_DRJ_CIRCLE-38  TGAATTTGATTAACACGATCAAAATCGCGCTGGGAAACAAATGATGGA...
CC_DRJ_CIRCLE-39  TGAATTTGATTAACACGATCAAAATCGCGCTGGGAAACAAATGATGGA...
CC_DRJ_CIRCLE-40  TGAATTTGATTAACACGATCAAAATCGCGCTGGGAAACAAATGATGGA...
MD_DRJ_CIRCLE-A  TGAATTTGATTAACACGATCAAAATCGCGCTGGGAAACAAATGATGGA...
MD_DRJ_CIRCLE-B  TGAATTTGATTAACACGATCAAAATCGCGCTGGGAAACAAATGATGGA...
MD_DRJ_CIRCLE-C  TGAATTTGATTAACACGATCAAAATCGCGCTGGGAAACAAATGATGGA...
MD_DRJ_CIRCLE-D  TGAATTTGATTAACACGATCAAAATCGCGCTGGGAAACAAATGATGGA...
MD_DRJ_CIRCLE-E  TGAATTTGATTAACACGATCAAAATCGCGCTGGGAAACAAATGATGGA...
MD_DRJ_CIRCLE-F  TGAATTTGATTAACACGATCAAAATCGCGCTGGGAAACAAATGATGGA...
MD_DRJ_CIRCLE-G  TGAATTTGATTAACACGATCAAAATCGCGCTGGGAAACAAATGATGGA...
MD_DRJ_CIRCLE-H  TGAATTTGATTAACACGATCAAAATCGCGCTGGGAAACAAATGATGGA...
MD_DRJ_CIRCLE-I  TGAATTTGATTAACACGATCAAAATCGCGCTGGGAAACAAATGATGGA...
MD_DRJ_CIRCLE-J  TGAATTTGATTAACACGATCAAAATCGCGCTGGGAAACAAATGATGGA...
MD_DRJ_CIRCLE-K  TGAATTTGATTAACACGATCAAAATCGCGCTGGGAAACAAATGATGGA...
MD_DRJ_CIRCLE-L  TGAATTTGATTAACACGATCAAAATCGCGCTGGGAAACAAATGATGGA...
MD_DRJ_CIRCLE-M  TGAATTTGATTAACACGATCAAAATCGCGCTGGGAAACAAATGATGGA...
MD_DRJ_CIRCLE-N  TGAATTTGATTAACACGATCAAAATCGCGCTGGGAAACAAATGATGGA...
MD_DRJ_CIRCLE-O  TGAATTTGATTAACACGATCAAAATCGCGCTGGGAAACAAATGATGGA...
  
```

### Host Integration Motif

```

CC_HIM_CIRCLE-1  CTAATTTTGGACAAACAAAGACCTGCTGGTGGAGGTAGTACAAT...
CC_HIM_CIRCLE-10  GGAAGATGTTTCACTGACACTAGTATAGTGGGTT...
CC_HIM_CIRCLE-11  TTAGTTTGGTTCACAAAGGGTAACTGGTATGACAT...
CC_HIM_CIRCLE-12  ATAAATTTGACATGAAAGACCTGAGTGGAGG...
CC_HIM_CIRCLE-13  ATAAATTTGACATGAAAGACCTGAGTGGAGG...
CC_HIM_CIRCLE-14  ATAAATTTGACATGAAAGACCTGAGTGGAGG...
CC_HIM_CIRCLE-15  ATAAATTTGACATGAAAGACCTGAGTGGAGG...
CC_HIM_CIRCLE-16  ATAAATTTGACATGAAAGACCTGAGTGGAGG...
CC_HIM_CIRCLE-17  ATAAATTTGACATGAAAGACCTGAGTGGAGG...
CC_HIM_CIRCLE-18  ATAAATTTGACATGAAAGACCTGAGTGGAGG...
CC_HIM_CIRCLE-19  ATAAATTTGACATGAAAGACCTGAGTGGAGG...
MD_HIM_CIRCLE-A  ATAAATTTGACATGAAAGACCTGAGTGGAGG...
MD_HIM_CIRCLE-B  ATAAATTTGACATGAAAGACCTGAGTGGAGG...
MD_HIM_CIRCLE-C  ATAAATTTGACATGAAAGACCTGAGTGGAGG...
MD_HIM_CIRCLE-D  ATAAATTTGACATGAAAGACCTGAGTGGAGG...
MD_HIM_CIRCLE-E  ATAAATTTGACATGAAAGACCTGAGTGGAGG...
MD_HIM_CIRCLE-F  ATAAATTTGACATGAAAGACCTGAGTGGAGG...
MD_HIM_CIRCLE-G  ATAAATTTGACATGAAAGACCTGAGTGGAGG...
MD_HIM_CIRCLE-H  ATAAATTTGACATGAAAGACCTGAGTGGAGG...
MD_HIM_CIRCLE-I  ATAAATTTGACATGAAAGACCTGAGTGGAGG...
MD_HIM_CIRCLE-J  ATAAATTTGACATGAAAGACCTGAGTGGAGG...
MD_HIM_CIRCLE-K  ATAAATTTGACATGAAAGACCTGAGTGGAGG...
MD_HIM_CIRCLE-L  ATAAATTTGACATGAAAGACCTGAGTGGAGG...
MD_HIM_CIRCLE-M  ATAAATTTGACATGAAAGACCTGAGTGGAGG...
MD_HIM_CIRCLE-N  ATAAATTTGACATGAAAGACCTGAGTGGAGG...
MD_HIM_CIRCLE-O  ATAAATTTGACATGAAAGACCTGAGTGGAGG...
  
```



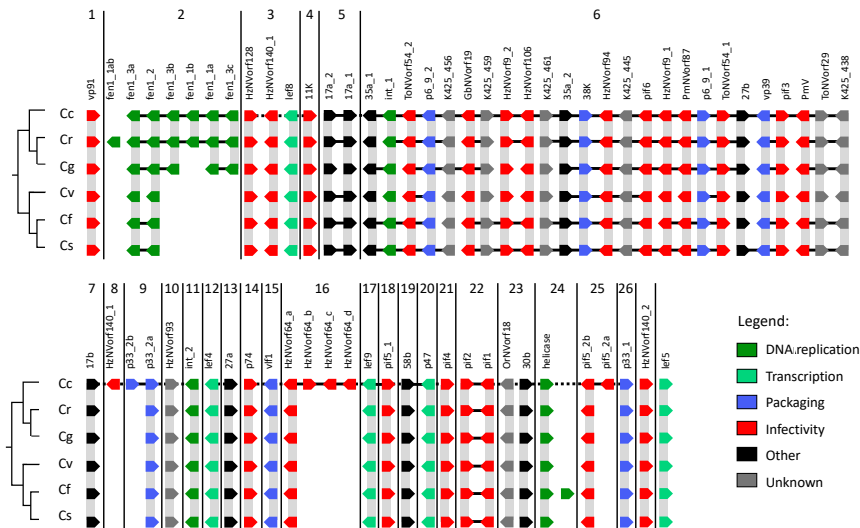
**Supplementary Figure 4. A** Schematic representation of the bracovirus production in wasp ovaries and their function in host cells. Circles from isolated loci, encoding in particular *ptp* and *Vank* genes, integrate into parasitized host DNA using HIM site mediated mechanism. **B** In purple framework, the alignment of Replication Unit Motifs (RUM) including *C. congregata* and *M. demolitor* sequences. In yellow framework, the alignment of the circle Direct Repeat Junctions (DRJ). In green framework, the alignment of the Host Integration Motifs (HIM).

A

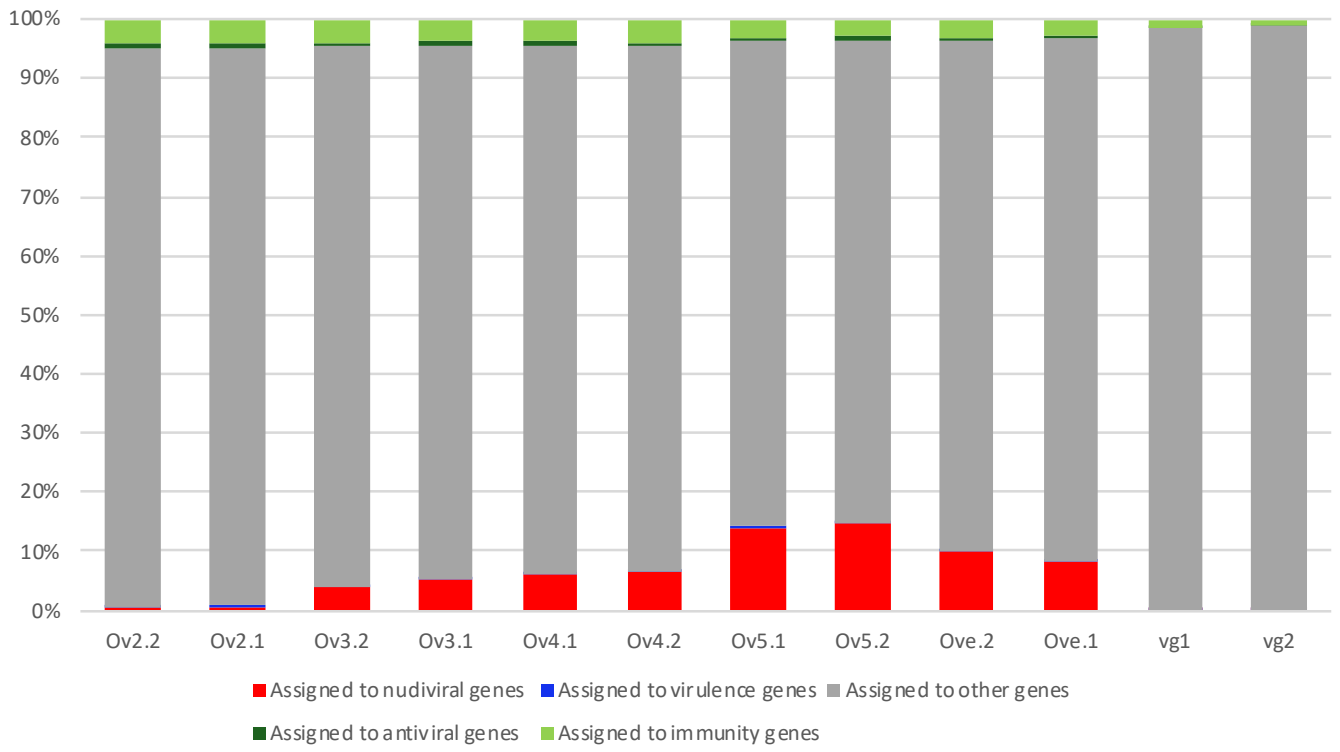
Protein function	Gene name	Gene content by species						dN/dS value	p-value
		C.c	Cr	C.g	C.v	C.f	C.s		
Replication, DNA processing	<i>helicase</i>	+	+	+	+	+	+	0.1343	< 0.001
	<i>int_1</i>	+	+	+	+	+	+	0.15141	< 0.001
	<i>int_2</i>	+	+	+	+	+	+	0.13921	< 0.001
	<i>fen-1-1a</i>	+	2	-	-	-	-	0.75876	0.284
	<i>fen-1-1b</i>	+	+	-	-	-	-	n.c.	n.c.
	<i>fen-1-2</i>	+	+	+	+	+	+	0.27467	< 0.001
	<i>fen-1-3a</i>	+	+	+	+	+	-	0.13039	< 0.001
	<i>fen-1-3b</i>	+	+	+	-	-	-	0.87961	0.555
	<i>fen-1-3c</i>	+	+	+	-	-	-	0.38875	< 0.001
Transcription	<i>p47</i>	+	+	+	+	+	+	0.05605	< 0.001
	<i>lef-8</i>	+	+	+	+	+	+	0.05973	< 0.001
	<i>lef-9</i>	+	+	+	+	+	+	0.05088	< 0.001
	<i>lef-4</i>	+	+	+	+	+	+	0.08525	< 0.001
	<i>lef-5</i>	+	+	+	+	+	+	0.38112	< 0.001
Packaging, assembly and release	<i>vif-1</i>	+	+	+	+	+	+	0.17119	< 0.001
	<i>vp91</i>	+	+	+	+	+	+	0.3808	< 0.001
	<i>vp39</i>	+	+	+	+	+	+	0.72163	0.057
	<i>p33_1</i>	+	+	+	+	+	+	0.17862	< 0.001
	<i>p33_2</i>	2	1	1	1	1	1	0.15432*	< 0.001
	<i>38K</i>	+	+	+	+	+	+	0.19847	< 0.001
	<i>p6.9_1</i>	+	+	+	+	+	+	0.08337	< 0.001
	<i>p6.9_2</i>	+	+	+	+	+	+	0.70662	0.267
per os infectivity factors and ODV envelope particle components	<i>p74</i>	+	+	+	+	+	+	0.79274	0.058
	<i>pif-1</i>	+	+	+	+	+	+	0.45494	< 0.001
	<i>pif-2</i>	+	+	+	+	+	+	0.319	< 0.001
	<i>pif-3</i>	+	+	+	+	+	+	0.71855	0.098
	<i>pif-4</i>	+	+	+	+	+	+	0.45842	< 0.001
	<i>pif-5_1</i>	+	+	+	+	+	+	1.10226	0.38
	<i>pif-5_2</i>	2	1	1	1	1	3	0.3709*	< 0.001
	<i>pif-6</i>	+	+	+	+	+	+	0.41774	< 0.01
	<i>HzNVorf9_1</i>	+	+	+	+	+	+	0.08198	< 0.001
	<i>HzNVorf9_2</i>	+	+	+	+	+	+	0.08558	< 0.001
	<i>GbNVorf19</i>	+	+	+	+	+	+	0.30979	< 0.001
	<i>HzNVorf64</i>	4	1	1	1	1	1	0.09716*	< 0.001
	<i>HzNVorf94</i>	+	+	+	+	+	+	0.11672	< 0.001
	<i>HzNVorf106</i>	+	+	+	+	+	+	0.08689	< 0.001
	<i>PmV 11K</i>	+	+	+	+	+	+	0.11206	< 0.001
	<i>HzNVorf128</i>	+	+	+	+	+	+	0.29473	< 0.001
	<i>HzNVorf140_1</i>	3	1	1	1	1	1	0.19362*	< 0.001
	<i>HzNVorf140_2</i>	+	+	+	+	+	+	0.1557	< 0.001
	<i>PmNVorf87</i>	+	+	+	+	+	+	0.34099	< 0.001
	<i>TaNVorf54_1</i>	+	+	+	+	+	+	0.245	< 0.001
	<i>TaNVorf54_2</i>	+	+	+	+	+	0.23574	< 0.001	
Other particle components	<i>17a_1</i>	+	+	+	+	+	+	0.98093	0.839
	<i>17a_2</i>	+	+	+	+	+	+	0.62831	< 0.05
	<i>17b</i>	+	+	+	+	+	+	0.11694	< 0.001
	<i>27a</i>	+	+	+	+	+	+	0.2348	< 0.001
	<i>27b</i>	+	+	+	+	+	+	0.24099	< 0.001
	<i>30b</i>	+	+	+	+	+	+	0.46248	< 0.001
	<i>35a_1</i>	+	+	+	+	+	+	0.74071	0.088
	<i>35a_2</i>	+	+	+	+	+	+	0.55692	< 0.001
	<i>58b</i>	+	+	+	+	+	0.58867	< 0.001	
Unknown	<i>K425_438</i>	+	+	+	+	+	+	0.66340	0.076
	<i>K425_445</i>	+	+	+	+	+	+	0.83681	0.45
	<i>K425_456</i>	+	+	+	+	+	+	0.14541	< 0.001
	<i>K425_459</i>	+	+	+	+	+	+	0.20317	< 0.001
	<i>K425_461</i>	+	+	+	+	+	+	0.14772	< 0.001
	<i>TaNVorf29</i>	+	+	+	+	+	+	0.15643	< 0.001
	<i>HzNVorf93</i>	+	+	+	+	+	+	0.18237	< 0.001
	<i>OrNVorf18</i>	+	+	+	+	+	0.38808	< 0.001	
odv-e66	<i>odv-e66-1</i>	+	+	+	+	+	+	0.57915	< 0.001
	<i>odv-e66-2</i>	+	+	+	+	+	+	0.84754	< 0.001
	<i>odv-e66-3</i>	+	+	+	+	+	+	0.51583	< 0.01
	<i>odv-e66-4</i>	+	+	+	+	+	-	0.53930	< 0.001
	<i>odv-e66-5</i>	+	+	+	+	+	-	0.71140	< 0.05
	<i>odv-e66-6/7/8/9</i>	4	1	1	3	1	2	n.c.	n.c.
	<i>odv-e66-10</i>	+	+	+	+	+	-	1.10867	0.589
	<i>odv-e66-11</i>	+	+	+	+	+	-	0.25798	< 0.001
	<i>odv-e66-12</i>	+	+	+	+	+	-	0.23769	< 0.001
	<i>odv-e66-13</i>	+	+	+	+	+	+	0.87336	0.439
	<i>odv-e66-14</i>	+	+	+	+	+	+	0.61298	< 0.01
	<i>odv-e66-15</i>	+	+	+	+	+	+	0.25491	< 0.001
	<i>odv-e66-16</i>	+	+	+	+	+	+	0.51120	< 0.001
	<i>odv-e66-17</i>	+	+	+	+	+	+	0.58245	< 0.001
	<i>odv-e66-18</i>	+	+	+	+	+	-	0.41734	< 0.001
	<i>odv-e66-19</i>	+	+	+	+	+	+	0.49926	< 0.001
	<i>odv-e66-20</i>	+	+	+	+	+	+	0.17390	< 0.001
	<i>odv-e66-21/22/23/24/25/26/27/28</i>	8	1	-	-	-	-	n.c.	n.c.
	<i>odv-e66-29</i>	+	+	+	+	+	2	0.36489	< 0.001
	<i>odv-e66-30</i>	+	+	+	+	+	-	0.85965	0.211
	<i>odv-e66-31</i>	+	+	-	-	-	-	n.c.	n.c.
	<i>odv-e66-32</i>	+	+	-	-	-	-	0.52025	< 0.001
	<i>odv-e66-33</i>	+	+	-	-	-	-	n.c.	n.c.
<i>odv-e66-34</i>	+	+	-	-	-	-	n.c.	n.c.	
<i>odv-e66-35</i>	+	+	-	-	-	-	n.c.	n.c.	
	<i>odv-e66-36</i>	+	+	-	-	-	n.c.	n.c.	

\* the closest orthologue among *C.congregata* duplications was used to estimate dN/dS  
n.c. - dN/dS was not estimated when orthologues and paralogues were not distinguishable

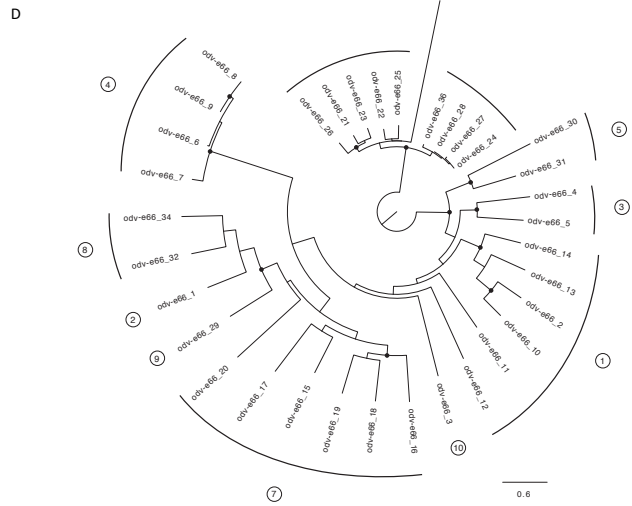
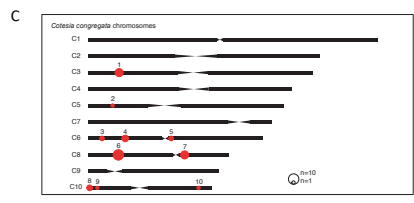
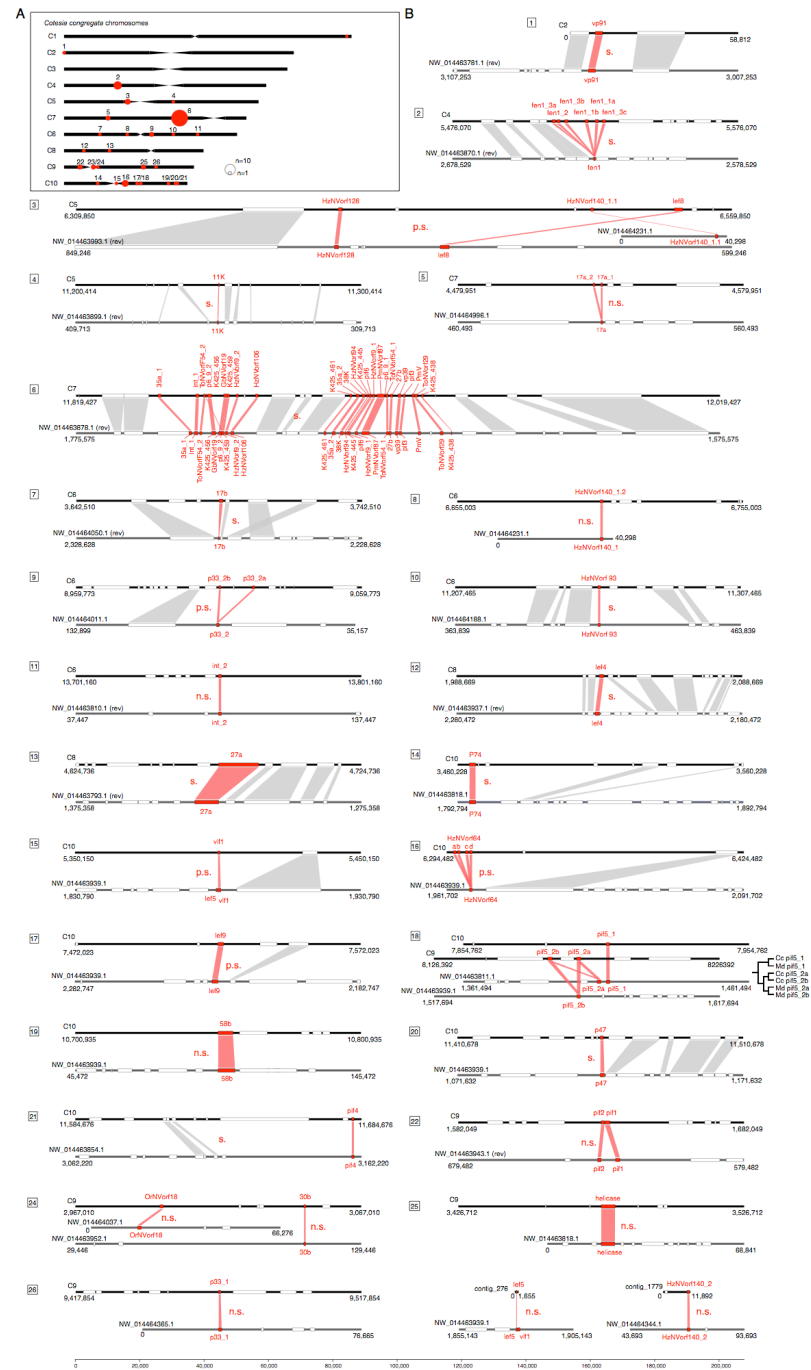
B



**Supplementary Figure 5. A** Evolutionary rates of nudiviral genes in *Cotesia* **B** Synteny of nudiviral genes across *Cotesia* species. Continuous black lines represent scaffolds and arrows indicate the orientation of the genes in each species. Number 1 to 26 correspond to the 26 nudiviral loci identified in *C. congregata* chromosomes. species (*C.c* = *C. congregata*; *C.r* = *C. rubecula*; *C.g* = *C. glomerata*; *C.v* = *C. vestalis*; *C.f* = *C. flavipes*; *C.s* = *C. sesamiae*; *M.d* = *M. demolitor*).



**Supplementary Figure 6.** Percentage of reads assigned to nudiviral, virulence or other genes out of the total number of reads assigned to *C. congregata* gene features.

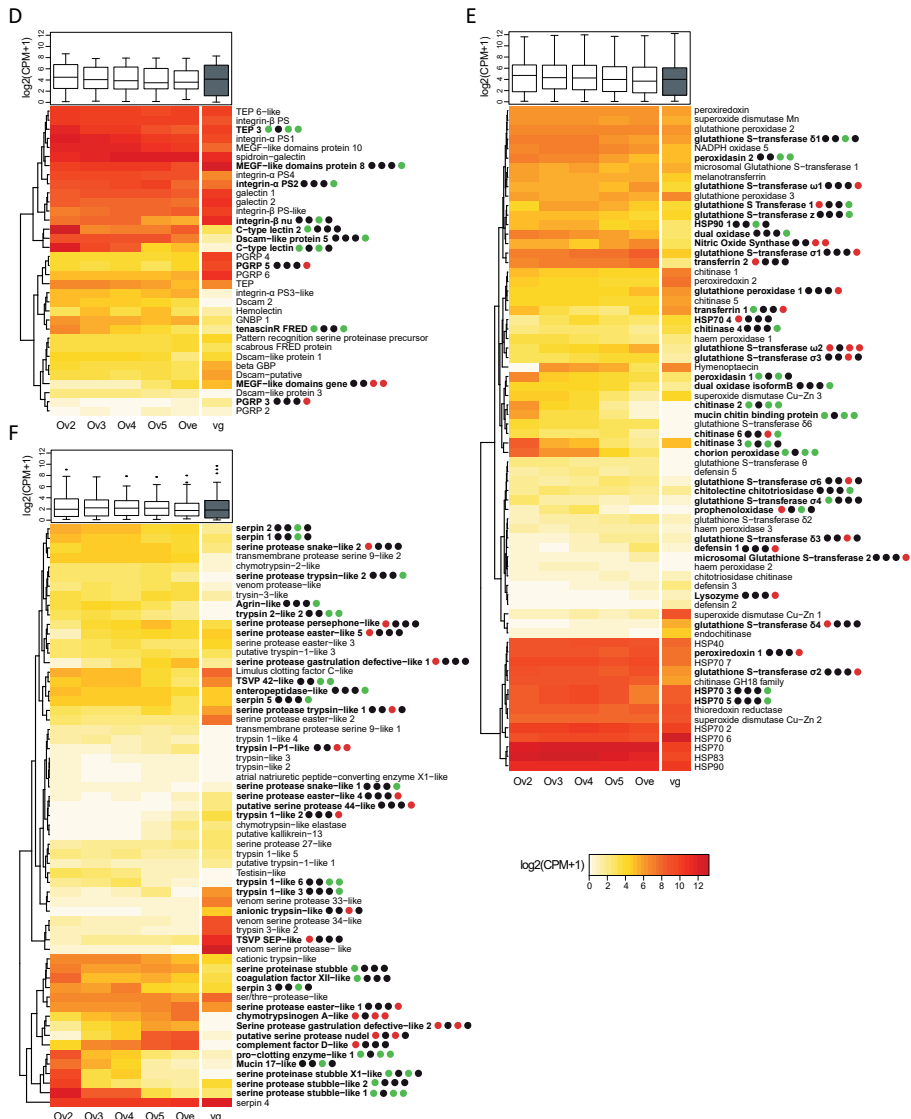
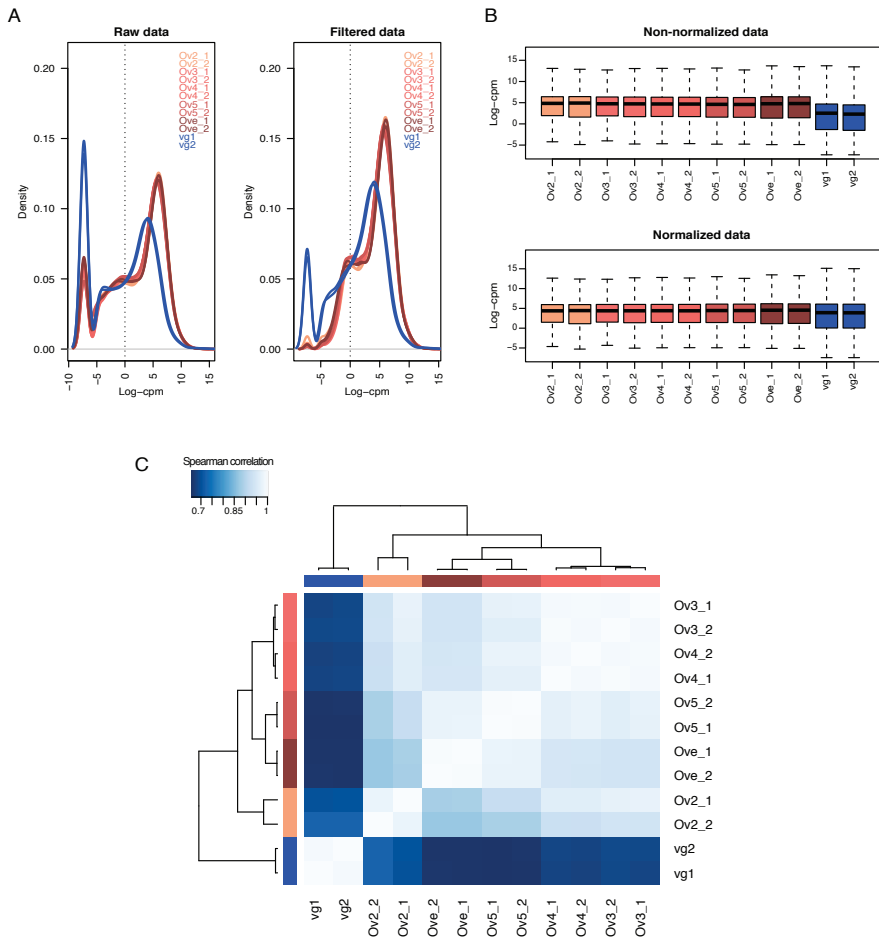


**Supplementary Figure 7.** Synteny between nudiviral genes containing regions of *C. congregata* and *M. demolitor*. **A** *C. congregata* chromosomes map. **B** Comparison of nudiviral genes regions of *C. congregata* and *M. demolitor*. To validate a synteny between the two specie (indicated by “s.” for synteny), we searched for at least two hymenopteran (non-viral) orthologous gene in the vicinity of homologous nudiviral gene(s) of the two species. If only one non-nudiviral orthologous gene was present we considered synteny as probable (“p.s.”: probable synteny). Finally, when no orthologous gene was present in the vicinity of the nudiviral gene(s) in the two species, we considered the regions containing nudiviral genes were not homologous (“n.s”: no synteny). *C. congregata* chromosomes and *M. demolitor* genome scaffolds are represented in black and dark grey respectively. Numbers 1 to 26 correspond to the 26 loci containing nudiviral genes identified in *C. congregata* chromosomes map. Red boxes indicate nudiviral genes and white boxes refer to hymenopteran genes. *M. demolitor* scaffolds for which the orientation is reversed compared to *C. congregata* chromosomes are indicated by “rev”. The scale shows length in bp. **C** Localization of nudiviral odv-e66 genes on *C. congregata* chromosomes. The 36 odv-e66 genes are clustered in 10 groups distributed in five different chromosomes of *C. congregata*. **D** Maximum-likelihood phylogeny of *C. congregata* odv-e66 family (1,000 bootstraps). Prior tree construction, the regions that were present in less than 50% of the aligned sequences were manually curated from the codon-based alignment and the odv-e66\_33 gene was excluded due to its short sequence. The tree was rooted to the midpoint and the black dots indicate nodes with at least 80% of support.





**Supplementary Figure 8.** Pie chart representations of gene ontology (GO) annotation results of *C. congregata* genome. GO hits were assigned to biological process, molecular function and cellular component. To facilitate visualization, only the 30 most abundant GO terms are shown for each category.



**Supplementary Figure 9.** Gene expression analysis of ovaries and venom glands of *Cotesia congregata*. **A** Density plots representing expression levels of all expressed genes (Raw data: 13,607 genes) and after filtering the genes that do not show CPM > 0.4 in at least 2 libraries on the 12 analyzed libraries (Filtered data: 11,216 genes). **B** Expression level distribution of the genes (filtered data) before and after CPM normalization using TMM method in edgeR. **C** Heatmap of Spearman correlation between the 12 analyzed libraries. The unsupervised clustering did not reveal discrepancies between biological replicates, then all libraries were retained for further analyses. Ov2, Ov3, Ov4 and Ov5 represent ovary samples collected at different larval stages. Ove and vg respectively refer to ovaries and venom glands from adult wasp. Heatmaps show the expression of the genes involved in **D** signal recognition, **E** signal transduction and **F** effector functions across the developmental stages of ovaries (Ov2, Ov3, Ov4, Ov5, Ove) and in venom glands (vg). The trees on the left are unsupervised hierarchical clustering of expression values. Boxplots represent overall expression of each immunity gene group in ovaries and venom glands. Bold names highlight the genes that are differentially expressed and dots represent the four different comparisons studied between consecutive ovary stages (Ov2 vs. Ov3, Ov3 vs. Ov4, Ov4 vs. Ov5 and Ov5 vs. Ove). Black, red and green dots indicate similar, increased and reduced expressions between consecutive developmental stages respectively.